Proposal to the MIT-Bates Linear Accelerator Center

Parity-Violating Quasielastic Electron Scattering on Deuterium at 120 MeV

The SAMPLE Collaboration

R. Carr, S. Covrig, B. W. Filippone, J. Gao, C. E. Jones,
T. M. Ito (spokesperson), J. W. Martin, R. D. McKeown, and B. Tipton
W. K. Kellogg Radiation Laboratory, Caltech

D. H. Beck and R. Hasty
University of Illinois

E. J. Beise, H. Breuer and D. T. Spayde
University of Maryland

A. Allen and M. Pitt
Virginia Polytechnic Institute

W. Korsch
University of Kentucky

T. Averett and J. Roche
College of William and Mary

B. Mueller
Argonne National Laboratory

S. P. Wells
Louisiana Tech University

D. Barkhuff, K. Dow, M. Farkhondeh, S. Kowalski, E. Tsentalovich, and T. Zwart
Bates Linear Accelerator Center, MIT

C. Crawford, D. Dutta, H. Gao, H. Kolster, N. Meitanos, H. Xiang,
F. Xiong, W. Xu, L. Y. Zhu, and V. Ziskin
Laboratory for Nuclear Science, MIT

G. Batigne, C. Furget, S. Kox, G. Quemener, J. -S. Real, and R. Tieulent
ISN Grenoble

Abstract

The previous two SAMPLE experiments yielded a measurement of the axial e-N form factor G_A^e substantially different from the theoretical estimate. One intriguing possible interpretation of this result is that the unexpected value of G_A^e is due to the nucleon's anapole form factor. In order to increase our confidence in this observation with a measurement that has an improved signal-to-background ratio, and hence has considerably different systematic effects, we propose to measure the parity-violating asymmetry in polarized quasielastic scattering from the deuterium at a lower beam energy of 120 MeV ($Q^2 \sim 0.04$ (GeV/c)^2). We request 110 coulombs of beam to measure the expected asymmetry of -2.07×10^{-6} with a statistical uncertainty of 0.38×10^{-6}. This will allow us to determine the axial e-N form factor G_A^e to $\delta G_A^e(T=1) = \pm 0.45(\text{stat.}) \pm 0.24(\text{sys.})$. Thus this measurement will provide a determination of G_A^e to a similar precision to the previous SAMPLE deuterium measurement with significantly different and smaller systematic effects.

Contents

1 Introduction **1**
- 1.1 Physics Motivation 1
- 1.2 Previous SAMPLE Measurements 2
- 1.3 Proposed Measurement 3

2 Physics Formalism **6**

3 Apparatus and Experimental Method **9**

4 Background **10**
- 4.1 Scintillation light yield 12
- 4.2 "Electromagnetic" shutter closed yield 15
- 4.3 "Neutron" shutter closed yield 15
- 4.4 Background summary 17

5 Uncertainties **17**
- 5.1 Overview 17
- 5.2 Statistical uncertainty 18
- 5.3 Systematic errors 20
- 5.4 Physics corrections 20
  - 5.4.1 Correction to the static approximation 20
  - 5.4.2 Deuteron elastic asymmetry and threshold electrodisintegration . . 21
- 5.5 Uncertainties summary 22

6 Summary **22**

7 Beam Request **22**

1 Introduction

1.1 Physics Motivation

Parity-violating electron scattering provides a unique probe of the electroweak structure of the nucleon. It has been well-established that elastic scattering studies yield new and interesting information on the strange vector matrix elements [1, 2]. This has been the basis for a substantial program of experiments at modern electron accelerator facilities, beginning with the SAMPLE experiment at MIT-Bates. As discussed below, the recent results from the successful running of SAMPLE indicate that the nucleon axial-vector coupling to the electron is substantially different from that expected from Z-exchange. This surprising result has generated new interest in the contribution from the anapole moment of the nucleon, which could provide an explanation for the SAMPLE observations. This new proposal to perform an additional measurement of the parity-violating asymmetry in quasielastic scattering from deuterium at 120 MeV is motivated by

1. increased interest in the nucleon's anapole moment that bears further experimental investigation,

2. the potential impact of a measurement of the deuteron asymmetry in kinematics with improved signal-to-background ratio as a means of increasing our confidence in the effects observed in previous runs at 200 MeV,

3. the window of opportunity afforded by the extended shutdown of South Hall running at Bates due to installation of the BLAST detector apparatus.

We note that no other backward-angle PV asymmetry measurements will become available for several years, so this represents an excellent opportunity for SAMPLE and MIT/Bates to make another key contribution to this subject.

While the subject of G_M^s has been discussed extensively in the literature [3], the axial e-N coupling has received much less attention. In general, we may write the axial e-N form factor as

$$G_A^e = G_A^Z + \eta F_A + R^e$$

where G_A^Z is the contribution from Z-exchange, η is a constant, F_A is the nucleon anapole moment, and R^e is a radiative correction (such as a Z-γ "box" amplitude). The constant η is given by

$$\eta = \frac{8\pi\sqrt{2}\alpha}{1 - 4\sin^2\theta_W} = 3.45.$$

The anapole moment is defined as the parity-violating coupling of the photon to the nucleon

$$-e\langle N|J^\mu_{\rm EM}|N\rangle \equiv -e\,\bar{u}_N\left\{F_1\gamma^\mu + F_2\frac{i\sigma^{\mu\nu}q_\nu}{2M_N} + F_A\,\left[G_F(q^2\gamma^\mu - q^\nu\gamma_\nu q^\mu)\gamma^5\right]\right\}u_N\,.$$

It is clear that the F_A term violates parity and should be due to weak interaction effects at the γ-N vertex. (Note that our definition of F_A differs from that used in the atomic physics literature by a factor of $m^2 G_F$ with the result that we expect the value of F_A to be of order unity.) Its effect should be small relative to $F_{1,2}$ (of order $m^2 G_F \simeq 10^{-5}$) but not zero. Contributions to the anapole moment were estimated by Musolf and Holstein [4] using a quark model of the nucleon, as well as π loops and ρ dominance. In contrast, the axial coupling to the neutrino can be written

$$G_A^\nu = G_A^Z + R^\nu$$

where the anapole does not contribute. Thus we see that parity-violating electron scattering can provide interesting and unique information on the axial vector structure of the nucleon.

1.2 Previous SAMPLE Measurements

At backward angles the parity-violating asymmetry for quasielastic scattering on the deuteron for the incident electron energy of 200 MeV in the static approximation can be written as

$$A_d = \left[\frac{0.049}{\sigma_d}\right]\left[\frac{-G_F Q^2}{\pi\alpha\sqrt{2}}\right]\left[1 - 0.22 G_A^e(T=1) - 0.10 G_M^s\right].$$

The similar expression for elastic electron scattering on the proton at 200 MeV is

$$A_p = \left[\frac{0.026}{\sigma_p}\right]\left[\frac{-G_F Q^2}{\pi\alpha\sqrt{2}}\right]\left[1 - 0.24 G_A^e(T=1) - 0.61 G_M^s\right].$$

G_F is the Fermi coupling constant and α is the fine structure constant. σ_d and σ_p are defined from $\sigma_{(p,n)} = \epsilon (G_E^{(p,n)})^2 + \tau (G_M^{(p,n)})^2$ and $\sigma_d = \sigma_p + \sigma_n$, where ϵ and τ are kinematic factors. The asymmetries are given in units of ppm and the form factors in units of nuclear magneton.

The previous two SAMPLE experiments measured the asymmetries for elastic scattering on the proton [5, 6, 7] and quasielastic scattering on the deuteron [8] for the incident electron energy of 200 MeV ($Q^2 = 0.1$ (GeV/c)^2).

The physics results of the previous SAMPLE runs are shown in Figure 1. The two error bands from the hydrogen experiment [7] and the (unpublished) preliminary deuterium experiment are indicated in the figure along with the estimate of the isovector axial e-N form factor $G_A^e(T=1)$ obtained by using the anapole form factor and radiative corrections of Musolf and Holstein [4]. Prior to running these experiments, the expected value of G_M^s was in the range -0.5 to 0, and the Musolf and Holstein value of $G_A^e(T=1) \simeq -0.71 \pm 0.20$. The experiments indicate a rather different picture as shown in Figure 1. The best value of G_M^s appears to be slightly positive, consistent with zero, and G_A^e is in substantial disagreement with the Musolf/Holstein estimate. One intriguing possibility is

that the unexpected value of G_A^e is due to the anapole form factor as defined above, and that the SAMPLE results are the first experimental evidence for this interesting quantity. Clearly the situation warrants further theoretical study as well as additional experimental investigation.

1.3 Proposed Measurement

We propose to use the SAMPLE apparatus to measure the parity-violating asymmetry on the deuteron at incident beam energy of 120 MeV ($Q^2 \sim 0.04$ (GeV/c)^2). At 120 MeV, the parity-violating asymmetry for quasielastic scattering on the deuteron at backward angles is

$$A_d = \left[\frac{0.028}{\sigma_d}\right]\left[\frac{-G_F Q^2}{\pi\alpha\sqrt{2}}\right][1 - 0.31 G_A^e(T=1) - 0.09 G_M^s]\,.$$

The similar expression for elastic electron scattering on the proton at 120 MeV is

$$A_p = \left[\frac{0.015}{\sigma_p}\right]\left[\frac{-G_F Q^2}{\pi\alpha\sqrt{2}}\right][1 - 0.33 G_A^e(T=1) - 0.49 G_M^s]\,.$$

As for 200 MeV, the deuteron asymmetry is mostly sensitive to the isovector axial form factor $G_A^e(T=1)$ and the deuteron asymmetry is larger than the proton asymmetry. We also note the increased sensitivity of the asymmetries to $G_A^e(T=1)$ compared to 200 MeV. At this lower beam energy, the deuteron asymmetry is smaller by a factor of three than it was in the earlier SAMPLE runs while the cross section is higher by a similar factor. As will be discussed in Section 4, the background in the detector will be similar to that seen at 200 MeV, yielding an improved signal-to-background ratio. The substantial progress we achieved in controlling small helicity-correlated beam effects gives us confidence that we can reliably measure the reduced asymmetry at 120 MeV. Thus, we will perform a measurement that should

- yield an asymmetry substantially different from our other measurements,
- explore a region of very different signal-to-background ratio,
- provide new information on the axial form factor $G_A^e(T=1)$ and, therefore, the nucleon anapole moment F_A.

In Figure 2, we plot as a function of the incident electron energy the necessary beam charge to achieve such a statistical accuracy that the deuterium asymmetry given by the measured $G_A^e(T=1)$ value corresponds to a 2 sigma deviation from the asymmetry given by $G_A^e(T=1) = -0.71$. It can be seen that as we go below 120 MeV, the required running time increases rather steeply. One could also consider making a measurement with hydrogen, and the behavior of the plot corresponding to Figure 2 is similar, but the required running time is significantly longer both because of the smaller figure of merit

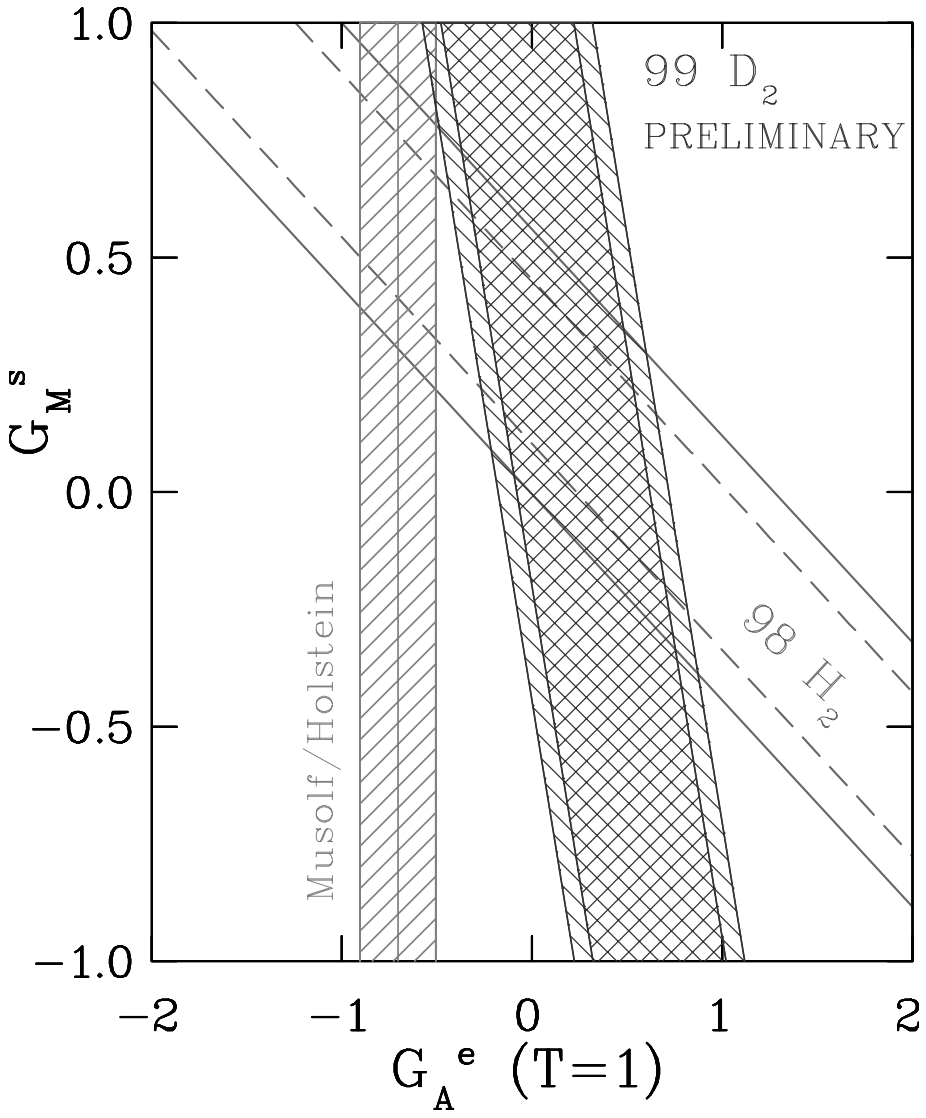

Figure 1: A result of a combined analysis of the data from the previous two SAMPLE measurements. The two error bands from the hydrogen experiment [7] and the (unpublished) preliminary deuterium experiment are indicated. The inner hatched region includes the statistical error and the outer represents the systematic uncertainty added in quadrature. The systematic error shown on the deuterium result is our estimate of the expected final value and the errors for the preliminary results are still under study. Also plotted is the estimate of the isovector axial e-N form factor $G_A^e(T=1)$ obtained by using the anapole form factor and radiative corrections of Musolf and Holstein [4].

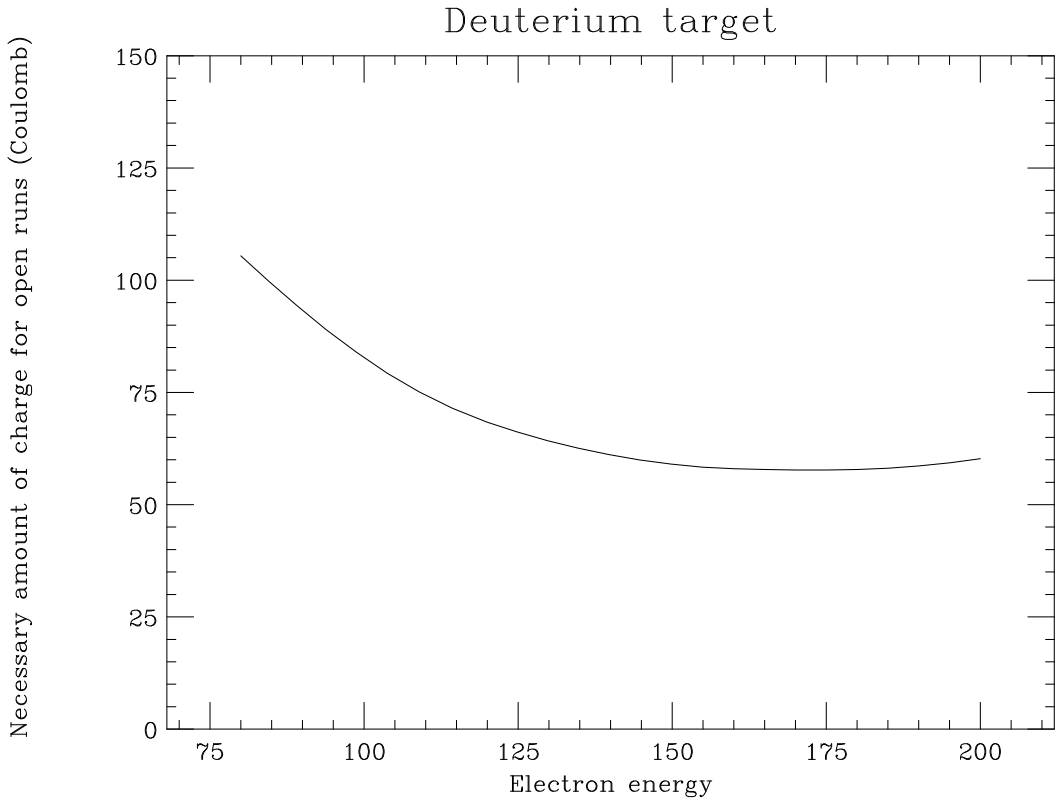

Figure 2: the necessary charge to achieve such a statistical accuracy that the deuterium asymmetry given by the measured $G_A^e(T=1)$ value corresponds to a 2 sigma deviation from the asymmetry given by $G_A^e(T=1) = -0.71$.

(both the asymmetry and the scattering cross section are smaller), and because of the substantial sensitivity of the hydrogen asymmetry to G_M^s.

In Figure 3, we plot the asymmetry for quasielastic scattering on the deuteron as a function of the incident electron energy for two different values of $G_A^e(T=1)$. The solid curve shows a projection of our 1999 preliminary deuterium asymmetry to lower Q^2. The dashed curve shows the asymmetry calculated with $G_A^e(T=1) = -0.71$ [4] and G_M^s determined from the combined analysis of the data from the previous two SAMPLE measurements. Our goal is to measure the parity-violating asymmetry to a statistical precision of 0.38 ppm, which corresponds to a 2 sigma deviation from the dashed line if the new result is consistent with our existing preliminary results. Note that the possible change in the values of G_A^e between 200 MeV ($Q^2 \sim 0.1$ (GeV/c)^2) and 120 MeV ($Q^2 \sim 0.04$ (GeV/c)^2) due the Q^2 dependence is expected to be negligibly small compared to the experimental error. Based on our experience from the previous two SAMPLE runs, we anticipate a final systematic error of approximately 0.16 ppm, as will be discussed further in Section 5.2.

2 Physics Formalism

We assume the standard model for electroweak interactions. The leptonic couplings are completely determined, and the hadronic couplings are expressed as form factors which are the objects to be studied by experiment.

The electromagnetic form factors can be designated F_1^γ and F_2^γ where the indices 1 and 2 refer to the usual Dirac form for the vector current

$$< N|V_\mu^{\rm EM}|N >= \overline{u}_N \left(F_1 \gamma_\mu + F_2 \frac{i\sigma_{\mu\nu} q^\nu}{2M_N} \right) u_N$$

The vector weak neutral current is expressed in an analogous fashion with the form factors F_1^Z and F_2^Z. In the discussion below we will use the linear combination of these known as the Sachs form factors: $G_E = F_1 - \tau F_2$ and $G_M = F_1 + F_2$, where $\tau = Q^2/(2M_N)^2$ with M_N being the nucleon mass. In addition, there is the neutral weak axial form factor G_A defined by

$$< N|A_\mu^{\rm NW}|N >= G_A \overline{u}_N \gamma_\mu \gamma_5 u_N.$$

There is also a contribution from the anapole term to the electromagnetic current:

$$< N|A_\mu^{\rm EM}|N >= \overline{u}_N F_A \left[G_F (q^2 \gamma^\mu - q^\nu \gamma_\nu q^\mu) \gamma^5 \right] u_N.$$

In the lowest order, the asymmetries for longitudinally polarized electrons scattering from unpolarized protons or neutrons are [9]

$$A_p = \left[\frac{-G_F Q^2}{4\pi\alpha\sqrt{2}} \right] \frac{\epsilon G_E^{\gamma,p} G_E^{Z,p} + \tau G_M^{\gamma,p} G_M^{Z,p} - (1 - 4\sin^2\theta_W) \epsilon' G_M^{\gamma,p} G_A^{e,p}}{\epsilon (G_E^{\gamma,p})^2 + \tau (G_M^{\gamma,p})^2} \qquad (1)$$

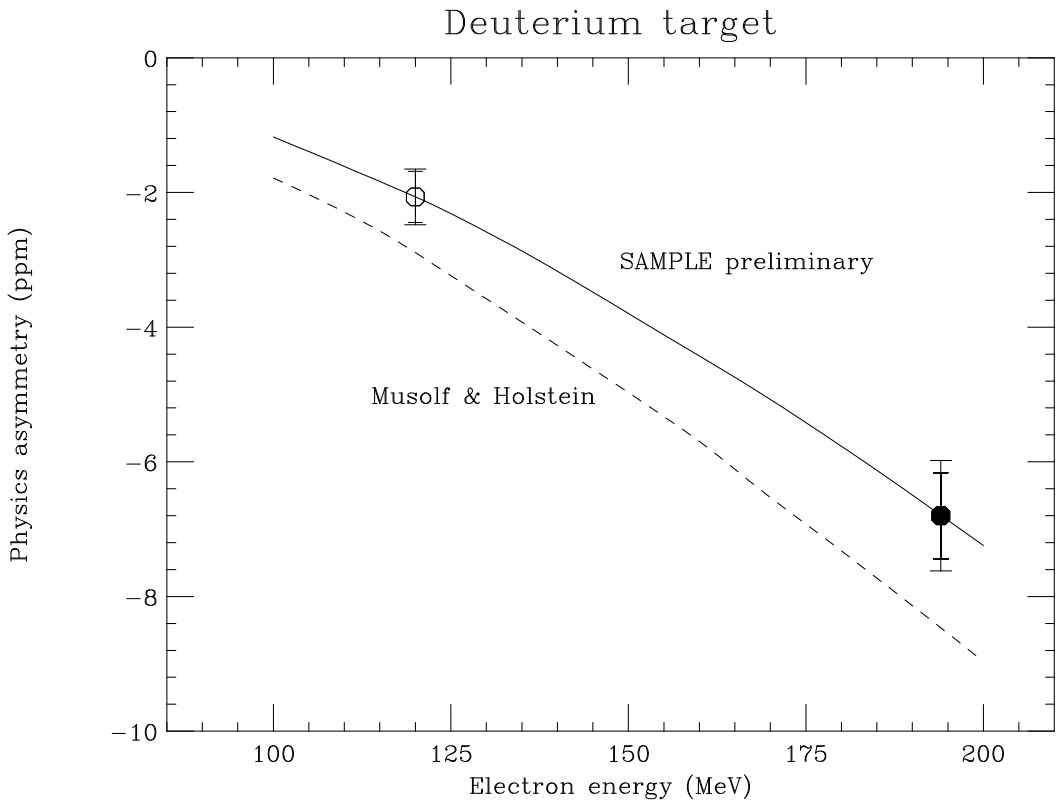

Figure 3: Deuterium asymmetry as a function of the incident electron energy for different values of G_A^e. The central value of G_M^s determined by the previous two SAMPLE measurements is assumed in constructing this plot. The preliminary result from the 1999 200 MeV deuterium run and the projected result from the proposed measurement are also shown. The two different error bars on each point correspond to the statistical error only and the statistical and systematic errors combined, respectively.

$$A_n = \left[\frac{-G_F Q^2}{4\pi\alpha\sqrt{2}}\right] \frac{\epsilon G_E^{\gamma,n} G_E^{Z,n} + \tau G_M^{\gamma,n} G_M^{Z,n} - (1-4\sin^2\theta_W)\epsilon' G_M^{\gamma,n} G_A^{e,n}}{\epsilon (G_E^{\gamma,n})^2 + \tau (G_M^{\gamma,n})^2} \tag{2}$$

where

$$\epsilon = \frac{1}{1+2(1+\tau)\tan^2\frac{\theta}{2}}$$

$$\epsilon' = \sqrt{\tau(\tau+1)(1-\epsilon^2)}$$

are kinematic quantities, Q^2 is the four-momentum transfer, and θ is the laboratory electron scattering angle. The $G_{(E,M)}^{\gamma,(p,n)}$ form factors are the usual electric and magnetic form factors of the proton and neutron. The neutral weak form factors of the proton and neutron are written as

$$G_{(E,M)}^{Z,p} = (1-4\sin^2\theta_W)[1+R_V^p]G_{(E,M)}^{\gamma,p} - [1+R_V^n]G_{(E,M)}^{\gamma,n} - [1+R_V^s]G_{(E,M)}^{s}$$

$$G_{(E,M)}^{Z,n} = (1-4\sin^2\theta_W)[1+R_V^p]G_{(E,M)}^{\gamma,n} - [1+R_V^n]G_{(E,M)}^{\gamma,p} - [1+R_V^s]G_{(E,M)}^{s}$$

$$G_A^e = -G_A\tau_3 + G_A^s + \eta F_A + R^e$$

where $\tau_3 = +1(-1)$ for the proton (neutron) and $\eta = 3.45$ is a constant. In the above expressions the $R_V^{(p,n,s)}$ and R^e denote electroweak radiative corrections. Note that the asymmetries arise both from the interference between the electromagnetic amplitude and the neutral weak amplitude and from a cross term between the electromagnetic vector (magnetic) coupling and the electromagnetic axial coupling, which has a form of $G_M^\gamma F_A$.

The electroweak radiative corrections to the vector form factors are relatively well known and known to have a small effect on the measured asymmetry. In contrast, the anapole form factor and the radiative corrections to the axial form factor are poorly known and are the subject of this proposed experiment.

The asymmetry for the deuteron can be estimated by making the "static" approximation – assuming that the deuteron consists of a noninteracting neutron and proton at rest. In that case, the quasielastic cross section can be estimated as the incoherent sum of neutron and proton cross sections, $\sigma_d = \sigma_p + \sigma_n$ and the asymmetry is

$$A_d = \frac{\sigma_p A_p + \sigma_n A_n}{\sigma_d}.$$

The adequacy of this approximation will be discussed in Section 5.4.1.

We also note that due to the fact that the SAMPLE detector has no energy resolution we must correct for other scattering processes on the deuteron. They are elastic scattering on the deuteron and threshold inelastic scattering. The size and error associated with making these corrections in described in more detail in Section 5.4.2.

3 Apparatus and Experimental Method

This experiment will use the same apparatus as the previous two SAMPLE measurements, which is currently installed in the North Hall, and the same beam monitoring systems and feedback systems instrumented along the beamline. Since they are described in detail in the proposals of the previous SAMPLE experiments [5, 8], we only give a brief account here with emphases on the new developments since then. Also we will discuss issues associated with operating the accelerator at a lower energy.

We will use a 120 MeV polarized electron beam with a typical current of 40 μA. The beam will be incident on the circulating liquid deuterium target. The liquid deuterium target is 40 cm long, and is part of a high flow-rate recirculating liquid deuterium system, with a heat exchanger to remove the 600 W of heat deposited by the electron beam.

Electrons scattered in backward angles will be detected by a large ($\sim$ 1.5 sr) solid angle air Čerenkov detector. The detector consists of ten large mirrors, each with ellipsoidal curvature to focus the Čerenkov light onto one of ten photomultiplier tubes (PMT's). Each PMT is 8 inches in diameter and is shielded from the target and room background by a cast lead shield. A remotely controlled light shutter can cover each PMT for the background measurements. One-eighth of the data will be taken with shutter closed to determine the fraction of signal that is not due to light (see Section 4).

The signals from detector, beam toroid monitors, and various other beam monitors will be integrated and digitized for every 25 μs long beam pulse. The parity-violating asymmetry A will be determined from the asymmetries in the ratio of integrated detector signal to beam intensity for left- and right-handed beam pulses.

The light fraction of the signal contains a contribution from non-Čerenkov sources in addition to contribution from (quasi)elastically scattered electrons (see Section 4). In order to determine the elastic component of the light signal, we will spend a small fraction of the beam time running with a lower beam current (nA range). At such a beam current we can use conventional pulse counting techniques and look for coincidences between the mirror signal and the signal from scintillators placed behind the mirrors, which will allow us to clearly identify electrons scattered from the target.

The polarized electron beam at Bates is generated via photoemission from unstrained GaAs by polarized laser light. The laser beam helicity for each pulse is determined by a $\lambda/4$ Pockels cell and will be randomly chosen for each of ten consecutive beam pulses; the complement helicities are then used for the next ten pulses. The asymmetry in the normalized detector yields will be computed for "pulse pairs" separated by 1/60 of a second to minimize systematic errors. The electron beam helicity relative to all electronic signals can be manually reversed by inserting a $\lambda/2$ plate in the laser beam. (We denote this configuration as $\lambda/2$= "IN" as opposed to $\lambda/2$= "OUT".) We will reverse the IN/OUT configuration every few days to minimize false asymmetries and test for systematic errors. The electron polarization will be measured using a Møller polarimeter system on the beam line. The collaboration requests that the present state of the polarized source be

maintained and not be altered for R&D work for other programs until after this proposed experiment is completed.

Helicity correlations of various beam parameters such as the intensity, position, and angle at the target in both transverse dimensions, the energy, and the "halo" will be monitored continuously during the experiment. Four lucite Čerenkov counters at $\sim 12^{\circ}$ will monitor luminosity and test for helicity dependence. These monitors will detect low Q^2 elastic scattering at forward angles and other soft electromagnetic radiation and should show negligible parity-violating asymmetry.

The beam intensity asymmetry will be reduced through an active feedback system. The beam-helicity-correlated beam-position asymmetry will be reduced through a feedback system which was newly implemented in the polarized electron source in 1998 [10]. This feedback system is composed of a tilted glass plate in the laser beam path and a piezoelectric transducer. By adjusting the tilt glass plate with helicity reversal, the first-order beam position asymmetry is reduced, resulting in improved quality of the data. In Figure 4 the helicity-correlated beam position difference taken from our 1998 data is shown for the piezoelectric feedback system on and off.

The detector signals will be corrected for the helicity-correlated beam parameter difference before the asymmetry is computed for pulse pairs. Then the physics asymmetry will be determined by correcting the measured asymmetry for background dilution and bremsstrahlung radiative energy loss effect (Section 5.2). The asymmetries from the ten mirrors will be computed individually and will be combined with proper weighting.

There are a few different options for operating the accelerator at 120 MeV. For the previous 200 MeV runs, Transmitters 1, 2, 5, and 6 were used, in which configuration, the vernier and the energy feedback system are connected to Klystron 9 (Transmitter 4) and Klystron 11 (Transmitter 5), respectively. The ECS system requires Klystron 12 to be on. To accelerate electrons up to 120 MeV, two transmitters are required. So, one option is to use only Transmitter 1, and 2 and 6, in which case the vernier and the energy feedback system have to be moved to Transmitter 1 or 2. The other option is to use Klystrons 9 and 10 also but back-phase Klystron 10. Which option is better is subject to a further study, which is expected to take about a week, but in principle there is no technical difficulty with operating the machine at 120 MeV.

4 Background

For our experiment, we define the signal to be events arising in the photomultiplier from electrons that have undergone quasielastic scattering, threshold electrodisintegration, and elastic scattering. Any other process that gives rise to a signal in the photomultiplier tubes is defined to be background.

As discussed in Section 3, the SAMPLE detector has no energy resolution and collects any photons that are emitted within the detector acceptance. In addition, radiation

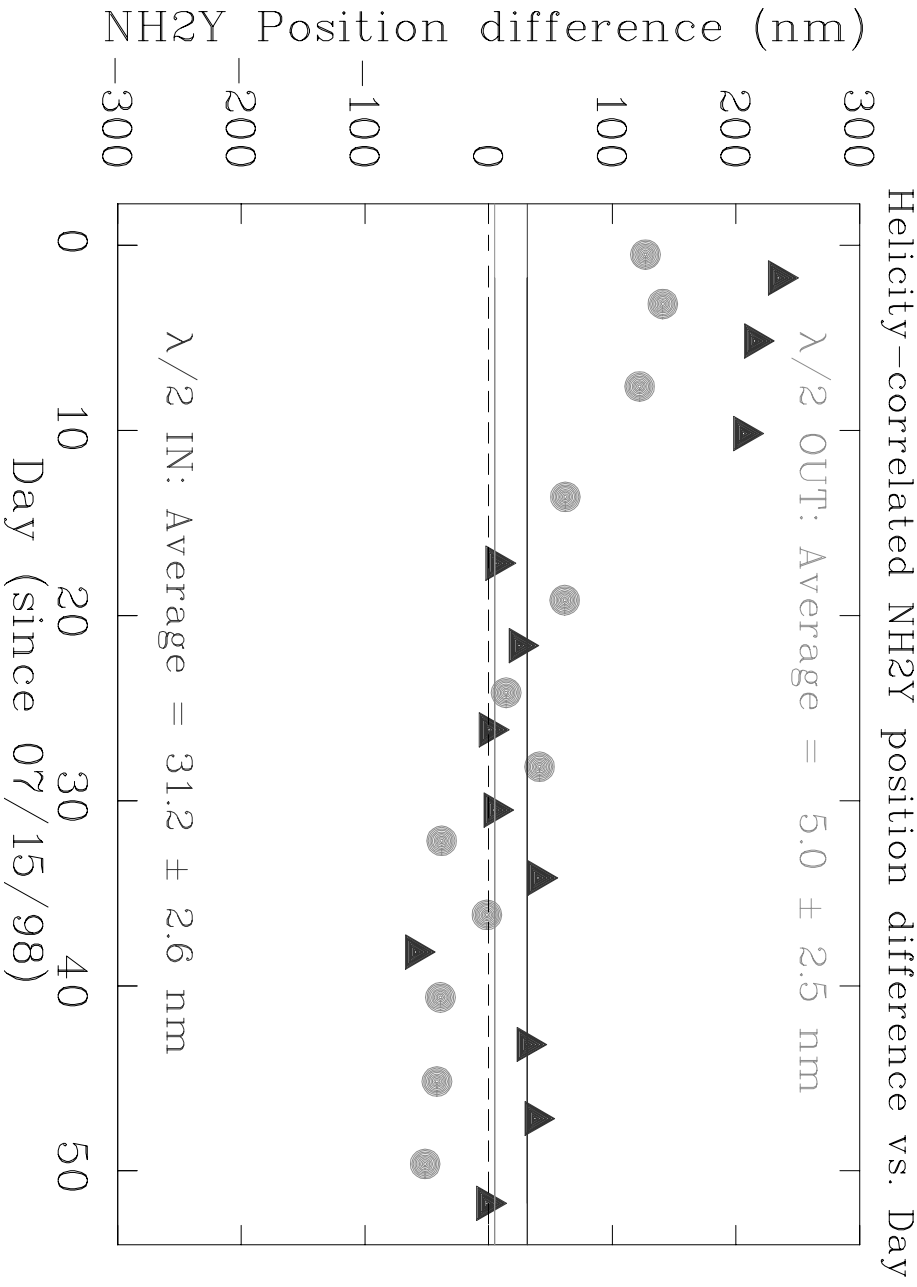

Figure 4: The helicity-correlated beam position difference with piezoelectric on and off. We ran for the first ten days or so with the piezoelectric feedback off.

which directly hits the photomultiplier tubes can also contribute to the signal output of the photomultiplier tubes.

The photomultiplier signal output yield can be divided into four pieces. First, it can be divided into the shutter closed yield and the light yield. The light yield is comprised of the part due to the Čerenkov light from the (quasi)elastically scattered electrons and the part that comes from scintillation light generated in the air. The shutter closed yield can also be divided into two components: one that results from low energy electromagnetic radiation which arises from showering in the target and scattering from downstream of the apparatus, and one that results from neutrons from photodisintegration in the target. In the following, we discuss our estimate of how the each piece of the background changes when we change the beam energy from 200 MeV to 120 MeV.

4.1 Scintillation light yield

The main sequence of processes contributing to this piece of background is as follows: 1) Incident electrons generate bremsstrahlung photons in the target. 2) Forward bremsstrahlung photons Compton scatter in the target in backward angles and come out into the detector volume as low energy (< 300 keV) photons. 3) These low energy photons are absorbed in the air in the detector volume and emission of scintillation light follows.

In order to estimate the level of this background, we calculated the energy spectrum of photons that come out of the scattering chamber for incident electron energy of 120 MeV and compared it with that calculated for incident electron energy of 200 MeV. Using GEANT, we passed an electron beam through the deuterium target and recorded the energy of each photon coming out of the scattering chamber for both incident electron energies of 120 MeV and 200 MeV. Figure 5 shows a comparison between these two spectra. They are very similar to each other both in shape and in magnitude.

Also we calculated the spectrum of energy deposition in the air in the volume between the mirrors and the detectors, which we believe to be a good representation of the amount of the emitted scintillation light, for both 120 MeV and 200 MeV. Using GEANT, we injected an electron beam into the target and recorded the energy deposition in the air in the volume between the mirrors and the detectors for each incident electron. These spectra are shown in Figure 6. Again, they are very similar both in shape and in magnitude.

From these plots, we conclude that the level of the background due to the scintillation in the air for the 120 MeV run will be the same as that of the 200 MeV run. This similarity in the background level can be understood by noting that the Bethe-Heitler formula for the bremsstrahlung cross section $d\sigma/d\nu$ (ν is the energy of photon emitted) is dominated by the term that is proportional to $1/\nu$ for low ν and this term has a very moderate dependence on the incident electron energy.

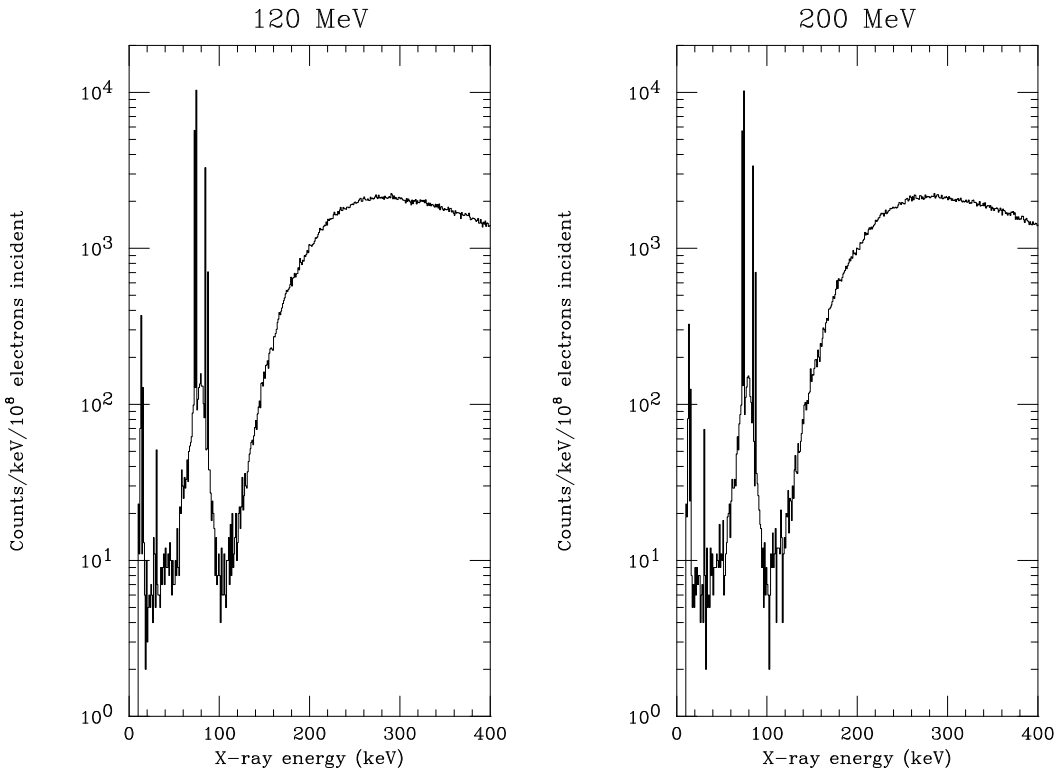

Figure 5: Comparison between the energy spectra of electrons coming out of the scattering chamber for incident electron energies of 120 MeV and 200 MeV

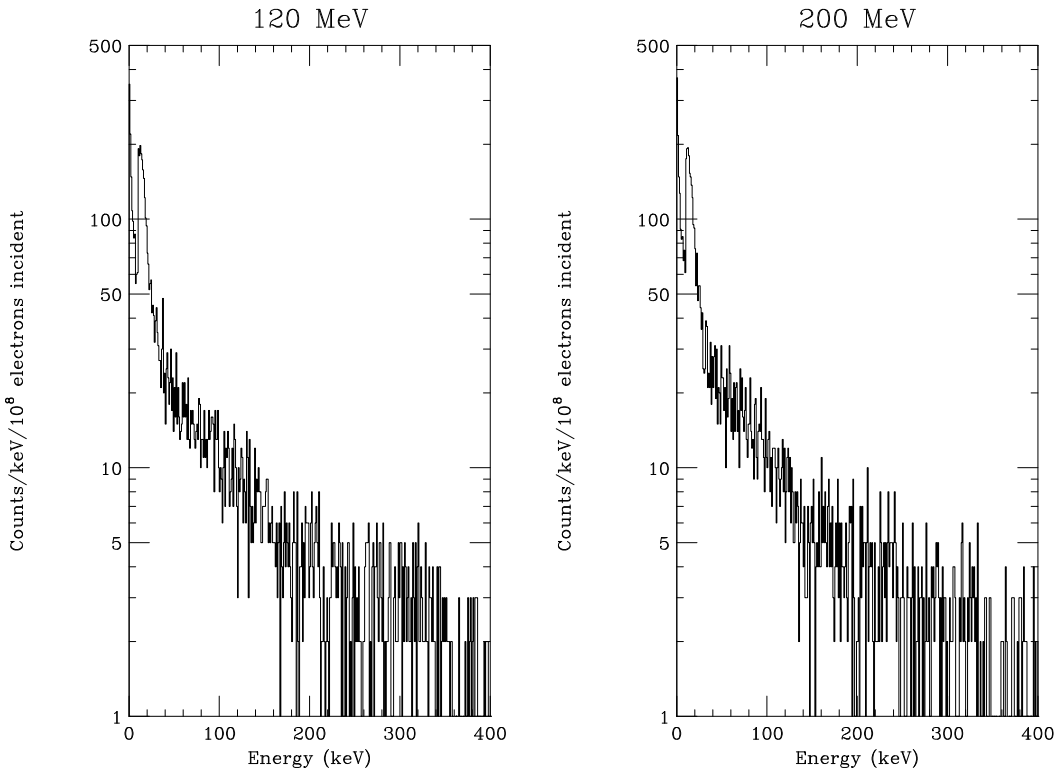

Figure 6: Comparison between the energy deposition spectra in the air in the volume between the mirrors and the detector for incident electron energies of 120 MeV and 200 MeV.

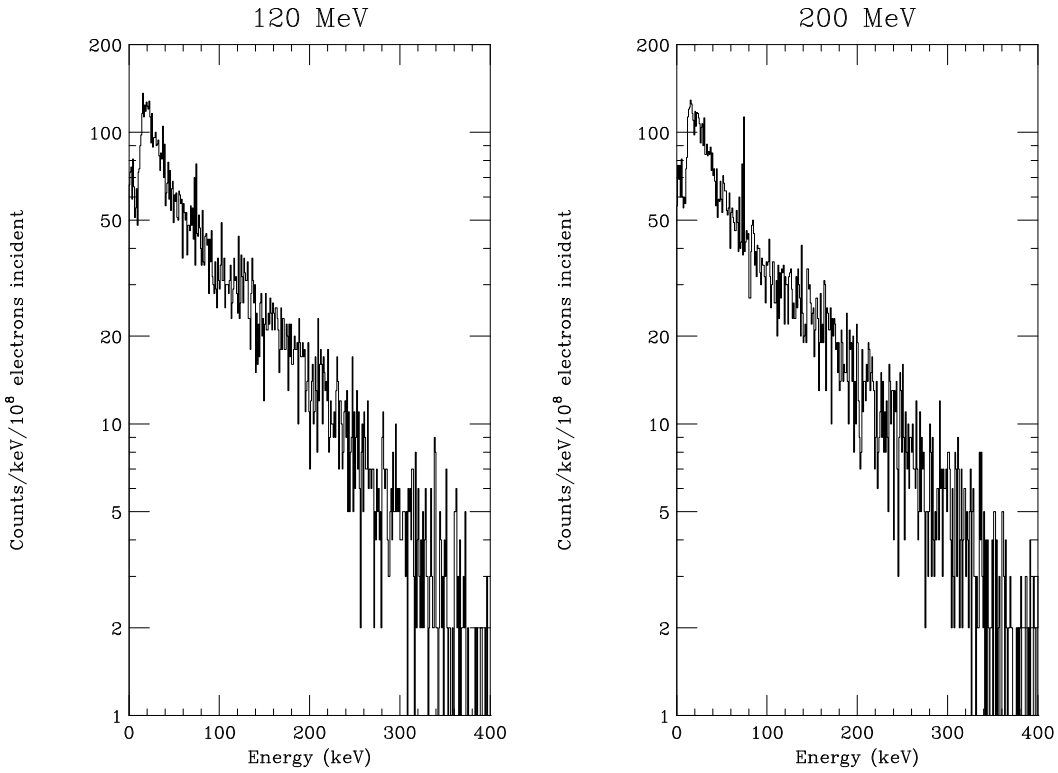

Figure 7: Comparison between the energy deposition spectra in the PMT's for incident electron energies of 120 MeV and 200 MeV.

4.2 "Electromagnetic" shutter closed yield

The origin of this background component is also bremsstrahlung in the target, so we can expect that the level of this background stays the same at 120 MeV just as the scintillation background. We calculated the spectra of energy deposition in the PMT's for incident electron energies of 120 MeV and 200 MeV. As for the scintillation light background estimation, we used GEANT, introducing a beam of electrons into the target and recording the energy deposition in the PMT's for each incident electron. Figure 7 shows the spectra calculated for incident electron energies of 120 MeV and 200 MeV. Again these two spectra are very similar, and we conclude that the electromagnetic shutter closed yield for 120 MeV is expected to be the same as that for 200 MeV.

4.3 "Neutron" shutter closed yield

In SAMPLE running at 200 MeV, the shutter closed normalized detector yield for deuterium was higher than for hydrogen. The difference is attributed to target-generated

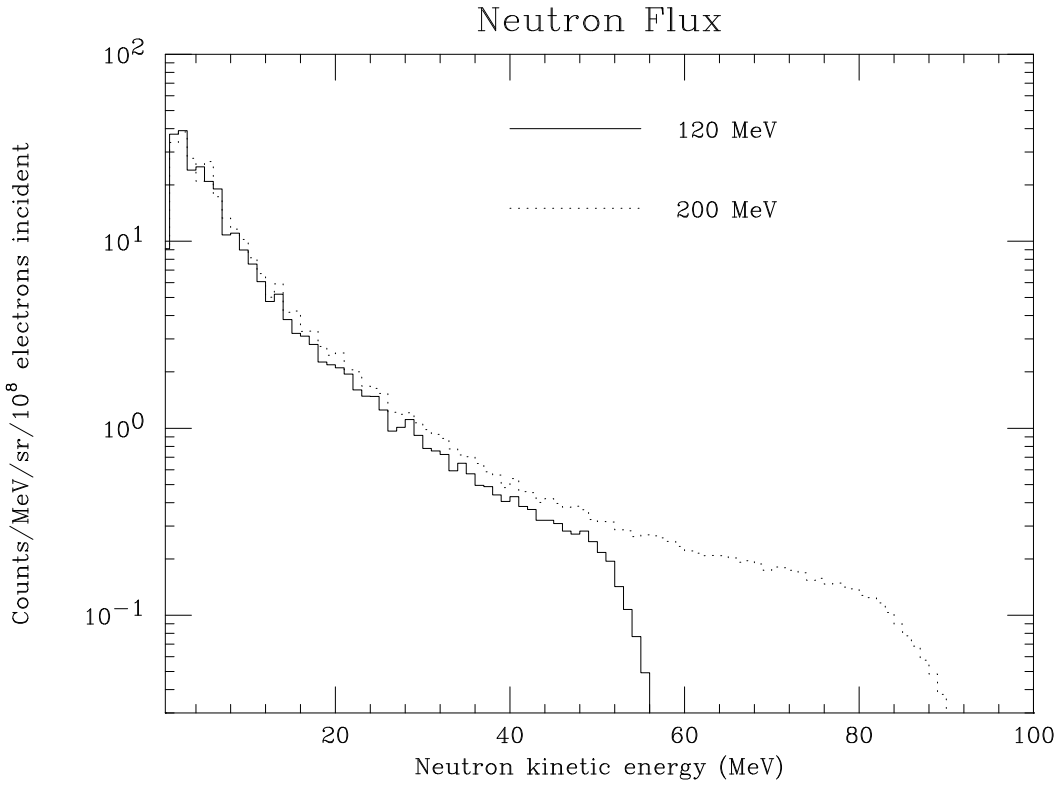

Figure 8: Comparison between the neutron energy spectra for incident electron energies of 120 MeV and 200 MeV.

neutrons interacting in the phototube and surrounding materials. The primary mechanism for generation of these neutrons is photodisintegration of the deuteron from electron beam bremsstrahlung. This background was kept to an acceptable level in the 1999 run by the installation of a 6 inch thick enclosure of borated polyethylene around the scattering chamber. It provided direct line-of-sight shielding between the target and phototubes, without any significant interference with the Cerenkov path of the scattered electrons.

To estimate the importance of this background at 120 MeV, we have done a GEANT simulation with the GCALOR interface, which provides a proper description of neutron interactions in the energy range of interest. Using known photodisintegration and bremsstrahlung generation cross sections, we generated the kinetic energy distribution of neutrons produced in the direction of the phototubes. We also put 6 inches of borated polyethylene in the simulation. The results for both 120 MeV and 200 MeV are shown in Figure 8. The shapes are similar, with the integrated yield being 7% higher for 200 MeV. The integrated yields and shape are similar for the same reason as in Section 4.1 - the weak energy dependence of the $1/\nu$ term in the Bethe-Heitler cross section.

4.4 Background summary

Since the major origin of all the different pieces of background is the bremsstrahlung radiation in the target, and the cross section for producing bremsstrahlung photons at low energies has a very moderate dependence on the incident electron energy, it is expected that the background level will be the same at 120 MeV as 200 MeV. On the other hand, the quasielastic cross section goes up by a factor of two. Therefore the expected values for the light fraction and the elastic fraction in the light signal are

$$f_{light} \sim 0.79$$

and

$$f_{elas} \sim 0.95.$$

5 Uncertainties

5.1 Overview

In order to extract the physics asymmetry due to the quasielastic scattering from the experimentally measured asymmetry, it is necessary to correct the measured asymmetry for the beam polarization, the bremsstrahlung radiative energy loss of the incident and scattered electrons, and the background dilution. Hence, the measured asymmetry and the physics asymmetry are related by the following expression:

$$A_{phys} = A_{measured} \times \frac{R_{rad}}{P_B \times D_B},$$

where R_{rad} is the asymmetry correction for electromagnetic radiative effects, P_B is the beam polarization, and $D_B (= \frac{S}{S+B})$ is the correction applied for the background dilution of the asymmetry. In SAMPLE experiment, D_B can be expressed as a product of two factors f_{light} and f_{elas} : $D_B = f_{light} \times f_{elas}$. As we discussed in Section 3, f_{light} is the light fraction of the signal yield, which is experimentally determined from the open-to-closed yield ratio, and f_{elas} is the (quasi)elastic scattering contribution to the light yield, which is determined by the pulsecounting method.

Furthermore, the physics asymmetry obtained using the above expression from the measured asymmetry has contributions from elastic scattering and threshold electrodisintegration in addition to the contribution from quasielastic scattering in which we are interested, *i.e.,*

$$A_{phys} = \frac{A_{QE}\left(\frac{d\sigma}{d\Omega}\right)_{QE} + A_{El}\left(\frac{d\sigma}{d\Omega}\right)_{El} + A_{TED}\left(\frac{d\sigma}{d\Omega}\right)_{TED}}{\left(\frac{d\sigma}{d\Omega}\right)_{QE} + \left(\frac{d\sigma}{d\Omega}\right)_{El} + \left(\frac{d\sigma}{d\Omega}\right)_{TED}}.$$

A correction must be made to the physics asymmetry in order to extract the quasielastic asymmetry (Section 5.4).

In the following, we examine each of the above mentioned factors, and discuss the projected uncertainty on A_{phys} and G_A^e.

5.2 Statistical uncertainty

The statistical uncertainty for the 120 MeV run was estimated utilizing the data from the 200 MeV deuterium run. The total detector yield normalized to a certain amount of charge (which we take to be 1 nC) for shutter open runs and shutter closed runs ($Y^{open}_{200\mathrm{MeV}}$ and $Y^{closed}_{200\mathrm{MeV}}$) can be obtained directly from the data. Also obtained directly from the data are the widths of the distributions of asymmetries formed by each pulse pair for both open and closed runs ($\delta A^{open}_{200\mathrm{MeV}}$ and $\delta A^{closed}_{200\mathrm{MeV}}$). From these, one can obtain the light yield ($Y^{light}_{200\mathrm{MeV}}$) and the width of the light yield asymmetry ($\delta A^{light}_{200\mathrm{MeV}}$) using the following relation:

$$(Y^{open})^2\ (\delta A^{open})^2 = (Y^{closed})^2\ (\delta A^{closed})^2 + (Y^{light})^2\ (\delta A^{light})^2. \qquad (3)$$

In order to estimate the statistical uncertainty for the 120 MeV, one has to know $\delta A^{open}_{120\mathrm{MeV}}$. As we have seen in Section 4, the shutter closed yield at the 120 MeV is estimated to be the same as 200 MeV. Hence, $Y^{closed}_{120\mathrm{MeV}} = Y^{closed}_{200\mathrm{MeV}}$ and $\delta A^{closed}_{120\mathrm{MeV}} = \delta A^{closed}_{200\mathrm{MeV}}$. For the light yield and the light yield asymmetry width, we can assume

$$Y^{light}_{120\mathrm{MeV}} = Y^{light}_{200\mathrm{MeV}} \times \frac{\sigma_{120\mathrm{MeV}}}{\sigma_{200\mathrm{MeV}}},$$

and

$$\delta A^{light}_{120\mathrm{MeV}} = \delta A^{light}_{200\mathrm{MeV}} \times \sqrt{\frac{\sigma_{200\mathrm{MeV}}}{\sigma_{120\mathrm{MeV}}}}.$$

since the light yield is dominated by the contribution from the (quasi)elastically scattered electrons ($f_{light} \sim 0.91$ for the 200 MeV deuterium run and it is estimated that $f_{light} \sim 0.955$ for the 120 MeV deuterium run). Then, using Eq. (3), $\delta A^{open}_{120\mathrm{MeV}}$ can be obtained. The yields and asymmetry widths obtained from the 200 MeV data and those estimated for the 120 MeV run are listed in Table 1. The statistical uncertainty is then estimated by

$$\delta A_{stat} = \frac{R_{rad}}{P_B \times D_B} \times \frac{\delta A^{open}_{120\mathrm{MeV}}}{\sqrt{C/C_0}},$$

where C is the total charge delivered for shutter open runs and C_0 is the amount of charge in a pulse pair (=133 nC).

In Figure 9, we plot the estimated statistical uncertainty as a function of charge delivered for the open shutter running. Our proposal is to run for 95 coulombs with shutter open.

Table 1: The yields and asymmetry widths obtained from the 200 MeV data and those estimated for the 120 MeV run. The yields are given in units of photoelectrons per nC, and the asymmetry widths are normalized to a pulse pair.

Energy	Y^{open}	δA^{open}	Y^{closed}	δA^{closed}	Y^{light}	δA^{light}	$\left(\frac{d\sigma}{d\Omega}\right)_{QE}$
200 MeV	4680	0.35×10^{-2}	1585	0.79×10^{-2}	3095	0.34×10^{-2}	52 nb/sr
120 MeV	7419	0.26×10^{-2}	1585	0.79×10^{-2}	5834	0.25×10^{-2}	98 nb/sr

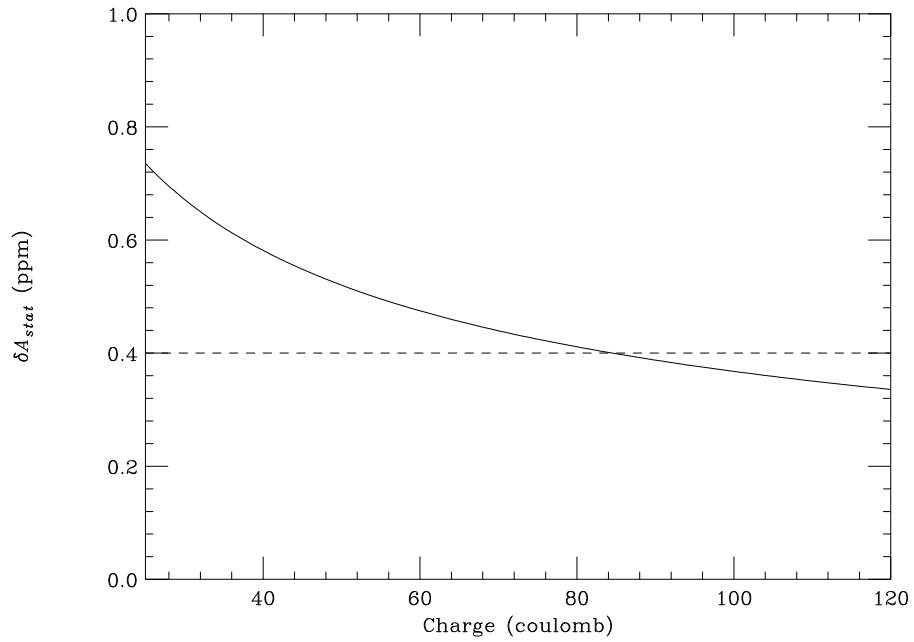

Figure 9: Estimated statistical uncertainty on the physics asymmetry as a function of the amount of charge delivered for the open shutter runs. The dashed line indicates the uncertainties corresponding to a 2 sigma measurement.

5.3 Systematic errors

We estimate the experimental systematic errors based on our experience with the previous two SAMPLE runs.

First of all, there is a systematic error on $A_{measured}$ that comes from the helicity-correlated corrections procedure we apply to the measured raw asymmetry. The total asymmetry correction to the 1998 hydrogen data was only 5% [7], and appears to be comparable in the 1999 deuterium data. We therefore estimate a 5% uncertainty for the proposed measurement(see Table 2).

In Reference [7], an uncertainty of 4% is assigned to the beam polarization determination. In 1999, a transmission polarimeter installed at the injector allowed daily monitoring of the beam polarization, resulting in fewer required Møller measurements. This reduced running overhead while allowing us to maintain a comparable total error in the beam polarization, so we expect a similar uncertainty for both the 1999 run and the proposed measurement here.

Another source of systematic uncertainties quoted in Reference [7] is the uncertainty from the unpolarized background dilution factor. An uncertainty of 4% is assigned to this factor. The dominant uncertainty in determining the dilution factor comes from the determination of f_{elas}. Since it is estimated that f_{elas} will be as high as 0.955 for the 120 MeV run, it can be expected that the uncertainty in dilution factor determination will be reduced. However, here we give a conservative estimate of 4% for the proposed measurement. The light fraction determination has a negligible contribution to the background dilution systematic error. Since we are expecting a higher light fraction, it is expected that a smaller closed running fraction is sufficient to determine the light fraction to the same accuracy as the previous experiments. We will run about 1/8 of the running time with the shutters closed.

5.4 Physics corrections

Corrections have to be made for the fact that the deuteron is not a free proton and neutron, as in the static approximation assumed in the introduction. There will also be elastic scattering from the deuteron and threshold electrodisintegration processes. Since the SAMPLE detector accepts all events down to Čerenkov energy threshold (21 MeV), we must correct for the contribution of these processes to the asymmetry. The size and the uncertainty of the corrections are estimated in the same way as Reference [8].

5.4.1 Correction to the static approximation

In developing the expression for the deuteron asymmetry in Section 2, we assumed the "static" approximation, which takes the neutron and proton in the deuteron to be non-interacting and at rest. To determine the experimentally measured true asymmetry, one must average the "static" asymmetry over the quasielastic peak. The net effect is a

slightly smaller asymmetry because the quasielastic response is asymmetric on the high ω(energy transfer) side where the asymmetry is smaller. For this proposal we estimated this effect by using a y-scaling model and found that the correction to the quasielastic asymmetry is about 5%. The size of this correction is fairly independent of the scattering angle (within the detector acceptance) and the incident electron energy. This changes the measured quasielastic asymmetry -2.67 ppm $\rightarrow -2.53$ ppm for the value of $G_A^e(T=1)$ given by the previous two SAMPLE experiments and -3.63 ppm $\rightarrow -3.45$ ppm for the Musolf and Holstein value of $G_A^e = -0.71$ n.m.

Hadjimichael, Poulis, and Donnelly discuss the dependence of the quasielastic asymmetry on various models for the deuteron [11]. They conclude that nuclear uncertainties in modeling the parity-violating asymmetry are at the $1 \sim 2\%$ level.

5.4.2 Deuteron elastic asymmetry and threshold electrodisintegration

The deuteron PV elastic asymmetry was calculated by Pollock [12], which gives the following expression for the asymmetry at backward angles:

$$A_{El} = \frac{G_F Q^2}{4\pi\alpha\sqrt{2}} \left(4\sin^2\theta_W + \frac{2G_M^s}{\mu_d} F_T \right),$$

where F_T is the fraction of the elastic cross section due to magnetic scattering and μ_d is the deuteron magnetic moment. With the best value of G_M^s by the previous two SAMPLE measurements, we obtain $A_{El} = 5.28$ ppm. We assign a 20% uncertainty to this value for the purpose of estimating errors. The differential cross section averaged over the acceptance of the detector is calculated to be 10.3 nb/sr.

For deuteron electrodisintegration near threshold, the PV asymmetry has been calculated by Musolf and Donnelly [9]. They assume that the dominant transition is the M1 transition from the deuteron ground state $^3S_1(T=0)$ to the lowest-lying $^1S_0(T=1)$ state. They find

$$A_{TED} = -\frac{G_F Q^2}{\pi\alpha\sqrt{2}} \left[\left(\frac{1}{2} - \sin^2\theta_W \right) - \frac{v_T'}{v_T} (1 - 4\sin^2\theta_W) \left(\frac{M_N}{q} \right) \left(\frac{G_A^e(T=1)}{2G_M^{T=1}} \right) \right],$$

where v_T and v_T' are kinematic factors. The asymmetry has a dependence on $G_A^e(T=1)$, and we obtain $A_{TED} = -4.24$ ppm for the value of $G_A^e(T=1)$ given by the previous two SAMPLE measurements and $A_{TED} = -4.93$ ppm for the Musolf and Holstein value of $G_A^e(T=1) = -0.71$ n.m.

Data on threshold electrodisintegration near our kinematics were estimated by interpolating data taken by Simon *et al.* [13] and subtracting the contribution from quasielastic scattering. Averaging over the acceptance of our detector and integrating over a 5 MeV energy bin, we obtained a cross section of 11.8 nb/sr. We assign a 10% error to this cross section for the purpose of estimating errors.

Putting together the contributions from quasielastic scattering, elastic scattering and threshold electrodisintegration, the physics asymmetry is

$$\begin{aligned} A_{phys} &= \frac{A_{QE}\left(\frac{d\sigma}{d\Omega}\right)_{QE} + A_{El}\left(\frac{d\sigma}{d\Omega}\right)_{El} + A_{TED}\left(\frac{d\sigma}{d\Omega}\right)_{TED}}{\left(\frac{d\sigma}{d\Omega}\right)_{QE} + \left(\frac{d\sigma}{d\Omega}\right)_{El} + \left(\frac{d\sigma}{d\Omega}\right)_{TED}} \\ &= \frac{(-2.53)\times(98.0) + (5.28)\times(10.3) + (-4.24)\times(11.8)}{98.0 + 10.3 + 11.8} \end{aligned}$$

which gives $A_{phys} = -2.07$ ppm for the best SAMPLE value of G_A^e. For $G_A^e(T=1) = -0.71$ n.m., we obtain $A_{phys} = -2.89$ ppm.

5.5 Uncertainties summary

The expected asymmetries, statistical and systematic uncertainties are summarized in Table 2. The values for the 200 MeV deuterium run are also listed for comparison. The statistical uncertainty assumes 95 coulomb of shutter open production running. Values for the systematic uncertainties due to the helicity-correlated correction procedure, the background dilution factor, and the beam polarization determination were taken from the analysis of the 200 MeV hydrogen data [7].

Expected uncertainties on $G_A^e(T=1)$ are summarized in Table 3. We expect to achieve $\delta G_A^e(T=1) = \pm 0.51$ n.m. from this measurement.

6 Summary

We propose to measure the parity-violating asymmetry in quasielastic scattering from deuterium at $Q^2 \sim 0.04$ (GeV/c)^2. With a production run of 110 coulombs, this will allow us to determine $G_A^e(T=1)$ to a similar precision to the previous SAMPLE deuterium run with significantly different systematic effects.

7 Beam Request

We request a total of 60 days of beam time, broken down into the categories shown in Table 4. This estimate is based on the assumption that running at 40 μA, two coulombs of data are written to tape per day. Note that this request does not include the possible time necessary to establish the "SAMPLE quality" beam. It is conceivable that the use of a combination of transmitters different from the 200 MeV tune can result in different effects on, for example, the beam halo, and hence different background characterestics. The collaboration would like to request about a week of beam time to check up the quality of the beam, a month or two ahead of the run, to allow a sufficient time for improvements, if needed.

Table 2: Summary of the uncertainties on the physics asymmetry. The expected asymmetries and projected uncertainties are listed for the proposed measurement. Also listed for comparison are the measured asymmetry in the 1999 200 MeV deuterium run and the uncertainties assigned to the asymmetry. Note: figures with (*) are taken from the analysis of 1998 hydrogen data. Similar values are expected for the 1999 deuterium data.

	200 MeV deuterium	120 MeV deuterium
$A^{open}_{measured}$	-1.33 ± 0.14 ppm	-0.530 ± 0.097
$A^{closed}_{measured}$	0.52 ± 0.56 ppm	0.0 ± 0.75
A_{phys}	$-6.69 \pm 0.64 \pm 0.51$ ppm	$-2.07 \pm 0.38 \pm 0.16$
P_B	36%	36%
R_{rad}	1.09	1.07
f_{light}	0.66	0.79
f_{elas}	0.91	0.95
$\delta A_{sys}/A$	7.5%(*)	7.5%
Systematic error breakdown		
Helicity-correlated corrections procedure	5%(*)	5%
Unpolarized background dilution factor	4%(*)	4%
Beam polarization determination	4%(*)	4%

Table 3: Summary of the uncertainties on G^e_A

Source	δG^e_A
Statistical	0.45
Experimental systematic uncertainty	0.19
δG^s_M	0.10
Other form factor uncertainties	0.05
Correction for elastic asymmetry	0.07
Correction for threshold electrodisintegration	0.05
Deuteron model uncertainty	0.05
Total	0.51

Table 4: Beam request

Item	Request	Beam parameters
Pulse counting measurements	10 shifts	120 MeV, < 1 μA, polarized e^-
Empty target studies	5 shifts	120 MeV, 40 μA, polarized e^-
Production run total	55 days	120 MeV, 40 μA, polarized e^-
Production run (shutter open)	95 Coulombs	
Production run (shutter closed)	15 Coulombs	

References

[1] R. D. McKeown, Phys. Lett. **B219**, 140 (1989).

[2] D. H. Beck, Phys. Rev. D **39**, 3248 (1989).

[3] R. D McKeown, In Parity Violation in Atoms and Polarized Electron Scattering, B. Frois and M.-A. Bouchiat (editors), World Scientific, Singapore, 423 (1999).

[4] M. J. Musolf and B. R. Holstein, Phys. Lett. **65**, 694 (1990).

[5] Bates Proposal #89-06, R. D. McKeown and D. H. Beck, spokespersons.

[6] B. Mueller *et al.*, Phys. Rev. Lett. **78**, 3824 (1997).

[7] D. T. Spayde *et al.*, Phys. Rev. Lett. , (2000).

[8] Bates Proposal #94-11 (M. Pitt and E. J. Beise, spokespersons)

[9] M. J. Musolf and T. W. Donnelly, Nucl. Phys. **A546**, 509 (1992).

[10] T. Averett *et al.* Nucl. Instrum. Methods Phys. Res. Sect. A **438**, 246 (1999).

[11] E. Hadjimichael, G. I. Poulis, and T. W. Donnelly, Phys. Rev. C **45**, 2666 (1992).

[12] S. J. Pollock, Phys. Rev. D **42**, 3010 (1990).

[13] G. G. Simon, *et al.*, Nucl. Phys. **A324**, 277 (1979).